Article

Cell Reports

Starvation-Dependent Regulation of Golgi Quality Control Links the TOR Signaling and Vacuolar Protein Sorting Pathways

Graphical Abstract

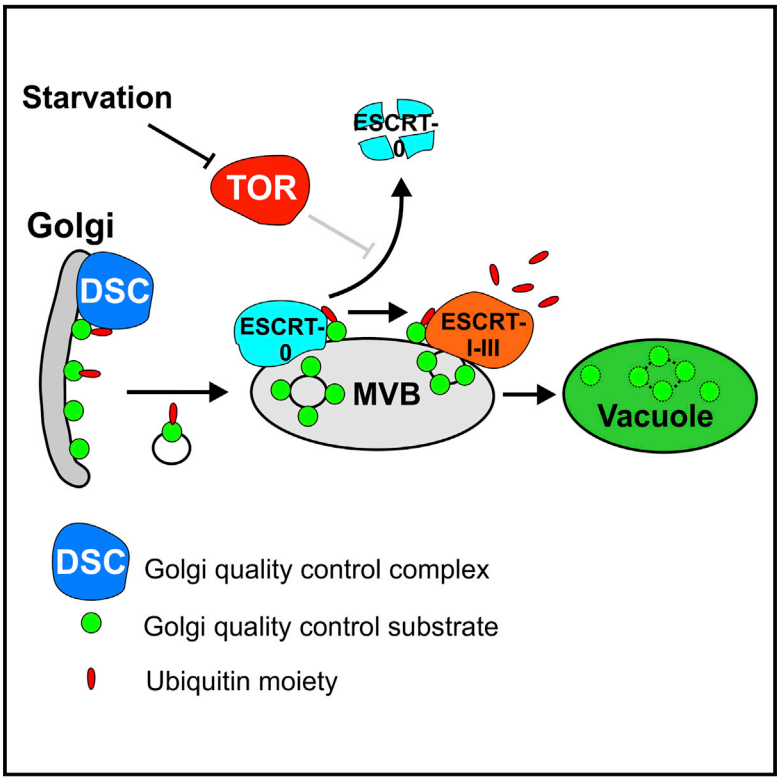

Authors

Niv Dobzinski, Silvia G. Chuartzman, Rachel Kama, Maya Schuldiner, Jeffrey E. Gerst

Correspondence

jeffrey.gerst@weizmann.ac.il

In Brief

Dobzinski et al. find that TOR inactivation upon starvation promotes delivery of Golgi proteins to the vacuole for degradation in yeast. Genetic screening identifies the defective-for-SREBP-cleavage (DSC) complex as mediating the ubiquitination of Golgi quality-control substrates that become recognized by the vacuolar protein sorting machinery upon TOR inactivation.

Highlights

- The DSC E3-ligase complex ubiquitinates Golgi quality-control (GQC) substrates
- TOR kinase turn-off facilitates the delivery of GQC substrates to the vacuole
- TOR regulates the proteasome-mediated degradation of ESCRT-0
- ESCRT-0 degradation directs GQC substrates to the multivesicular body and vacuole

Dobzinski et al., 2015, Cell Reports *12*, 1876–1886
September 22, 2015 ©2015 The Authors
http://dx.doi.org/10.1016/j.celrep.2015.08.026

OPEN ACCESS
CellPress

Cell Reports
Article

Starvation-Dependent Regulation of Golgi Quality Control Links the TOR Signaling and Vacuolar Protein Sorting Pathways

Niv Dobzinski,[1] Silvia G. Chuartzman,[1] Rachel Kama,[1] Maya Schuldiner,[1] and Jeffrey E. Gerst[1,*]
[1]Department of Molecular Genetics, Weizmann Institute of Science, Rehovot 76100, Israel
*Correspondence: jeffrey.gerst@weizmann.ac.il
http://dx.doi.org/10.1016/j.celrep.2015.08.026
This is an open access article under the CC BY-NC-ND license (http://creativecommons.org/licenses/by-nc-nd/4.0/).

SUMMARY

Upon amino acid (AA) starvation and TOR inactivation, plasma-membrane-localized permeases rapidly undergo ubiquitination and internalization via the vacuolar protein sorting/multivesicular body (VPS-MVB) pathway and are degraded in the yeast vacuole. We now show that specific Golgi proteins are also directed to the vacuole under these conditions as part of a Golgi quality-control (GQC) process. The degradation of GQC substrates is dependent upon ubiquitination by the defective-for-SREBP-cleavage (DSC) complex, which was identified via genetic screening and includes the Tul1 E3 ligase. Using a model GQC substrate, GFP-tagged Yif1, we show that vacuolar targeting necessitates upregulation of the VPS pathway via proteasome-mediated degradation of the initial endosomal sorting complex required for transport, ESCRT-0, but not downstream ESCRT components. Thus, early cellular responses to starvation include the targeting of specific Golgi proteins for degradation, a phenomenon reminiscent of the inactivation of *BTN1,* the yeast Batten disease gene ortholog.

INTRODUCTION

Nutrient starvation and environmental stress promote metabolic responses crucial for cell growth control and survival. The conserved TOR (target of rapamycin) Ser/Thr kinases are activated under nutrient-rich conditions and inhibited upon starvation, the latter leading to the induction of autophagy (Jung et al., 2010). Unlike mammalian cells that have one *TOR* gene (*mTOR*), budding yeast have two (*TOR1* and *TOR2*) that regulate growth and can be inhibited by rapamycin (Wullschleger et al., 2006). TOR effector signaling directly regulates a wide variety of essential processes, from protein synthesis to intracellular protein trafficking. As an example of the latter, TOR regulation of Npr1 kinase phosphorylation plays a major role in the sorting of yeast permeases (e.g., the high-affinity uracil permease, Fur4). Under nutrient-rich conditions, these permeases are targeted to the plasma membrane (PM), while they are delivered to the vacuole upon amino acid (AA) starvation or rapamycin treatment (i.e., TOR inactivation) from the PM, Golgi, and ER (Lauwers et al., 2010). Permease delivery to the vacuole upon starvation is important for maintaining a critical level of AAs essential for protein synthesis (and cell survival) early in starvation (Jones et al., 2012; Müller et al., 2015). Permease targeting for degradation necessitates ubiquitination by the Rsp5 E3 ligase and Npr1, which inhibits Art1, an arrestin-like adaptor that targets Rsp5 to substrates on the PM (MacGurn et al., 2011). Rsp5 is also involved in the ubiquitination and sorting of newly synthesized permeases from the Golgi to the vacuolar lumen via the vacuolar protein sorting/multivesicular body (VPS-MVB) pathway (Henne et al., 2011; Hurley, 2008; Lauwers et al., 2010). The ART-Rsp5 network may confer PM protein quality control (PMQC) and thus serve as a post-ER quality-control (post-ERQC) mechanism that directs unfolded/damaged proteins to the vacuole during proteotoxic stress (Zhao et al., 2013).

A post-ERQC mechanism proposed to operate at the level of the Golgi is Golgi quality control (GQC). Instead of Rsp5, the E3 ligase Tul1 ubiquitinates membrane proteins with transmembrane domains (TMDs) containing polar residues exposed to the lipid bilayer (e.g., unpalmitoylated Tlg1). This GQC mechanism identifies misfolded/damaged membrane proteins and directs them to the vacuole via the VPS pathway (Hettema et al., 2004; Reggiori and Pelham, 2002; Valdez-Taubas and Pelham, 2005). Interestingly, the *Schizosaccharomyces pombe* Tul1 ortholog, Dsc1, is part of a complex important for the proteasomal cleavage of sterol regulatory element-binding proteins (SREBPs) (Stewart et al., 2011). This defective-for-SREBP-cleavage (DSC) complex was identified in *Saccharomyces cerevisiae* (Ryan et al., 2012), although its function is unclear (Tong et al., 2014).

The delivery of ubiquitinated proteins from either the biosynthetic or endocytic pathways to the vacuole necessitates sorting into the MVB by the endosomal sorting complex required for transport (ESCRT), which is composed of four subcomplexes: ESCRT-0, -I, -II, and -III (Henne et al., 2011; Hurley, 2008). ESCRT-0 comprises Vps27 and Hse1, which bind to and cluster ubiquitinated cargos on endosomal membranes via ubiquitin-interacting motifs (UIMs: two on Vps27 and one on Hse1) and VPS27-Hrs-STAM domains (VHS: one on Vps27 and one on Hse1) (Bilodeau et al., 2002; Hirano et al., 2006; Wollert and Hurley, 2010). ESCRT-0 then recruits ESCRT-I (composed of Vps23, Vps28, Mvb37, and Mvb12) via Vps23, which binds to the same ubiquitin moieties as ESCRT-0 in order to convey the ubiquitinated

cargo (Bilodeau et al., 2003; Katzmann et al., 2003). However, the exact mode of temporal ESCRT regulation and their association with endosomal membranes is unclear (Morvan et al., 2012). Upon the interaction with ubiquitinated cargo, ESCRT-I recruits ESCRT-II (Vps22, Vps36, and Vps25) via an interaction between Vps28 and Vps36 to deform the membrane and recruit ESCRT-III monomers (Vps20, Snf7, Vps24, and Vps2) from the cytoplasm. Subsequently, Vps20 recruits Snf7, which oligomerizes and recruits Bro1 to stabilize the oligomers and Doa4 to deubiquitinate substrates prior to their entry into the MVB. ESCRT-III is released from the endosomal membrane to potentiate membrane invagination in a step catalyzed by the Vps4 AAA-ATPase and regulated by Ist1 (Shestakova et al., 2010).

Previously, we used yeast to model Batten disease, an early-onset neurodegenerative disorder that results from mutations in *CLN3*, a gene of unknown function. We determined that deletions in either *BTN1,* the yeast *CLN3* ortholog, or an ancillary gene, *BTN2*, led to the targeting of a specific subset of functional fluorescent-protein-tagged *trans* Golgi proteins (e.g., Yif1 and Kex2) to the endosome/vacuole. Thus, we proposed that Btn1 and Btn2 regulate selective endosome-Golgi protein retrieval and that Btn1 controls Golgi SNARE assembly (Kama et al., 2007, 2011). We now report that chronic AA starvation of wild-type (WT) yeast also redistributes GFP-Yif1 and other *trans* Golgi proteins to the vacuole. We show for the first time that TOR signaling acts (along with GQC) to control the fate of specific proteins that localize to the Golgi under normal nutrient-rich conditions but redistribute to the vacuole upon starvation/TOR inactivation. The intact *S. cerevisiae* DSC complex is shown to confer the ubiquitination of GQC substrates and to mark them for delivery to the vacuole via the MVB-VPS pathway. We also demonstrate that TOR signaling controls GQC by regulating ESCRT-0, as Vps27-Hse1 is targeted for degradation by the proteasome upon starvation and is necessary for the redistribution of GQC substrates. Our results link the GQC, DSC complex, MVB-VPS pathway, and proteasomal degradation to TOR signaling.

RESULTS

TOR Signaling Regulates the Steady-State Localization of *trans* Golgi Proteins

We observed that GFP-tagged Yif1 localized to the vacuole in control WT cells grown to stationary phase (i.e., chronic AA starvation; Figure S1A). Since starvation responses (e.g., autophagy) are mediated through the inhibition of TOR kinase activity (Jung et al., 2010), we examined whether the delivery of Yif1 to the vacuole is due to TOR inhibition. Therefore, we used rapamycin, a specific TOR inhibitor, or conditions of AA/nitrogen starvation in more controlled experiments. Upon the treatment of WT cells with either AA starvation or rapamycin (200 μg/l), we observed that GFP-Yif1 lost its typical Golgi patterning (i.e., small puncta) and was redistributed to the vacuole within ~100 min and 1 hr, respectively (Figure 1A). In contrast, no significant change in localization was observed in non-treated cells. To verify that GFP-Yif1 is degraded in the vacuole, we employed a *PEP4* deletion strain (*pep4*Δ) that is deficient in vacuolar hydrolase activity. In contrast to WT cells, GFP-Yif1 was not significantly degraded within 2 hr upon AA starvation in *pep4*Δ cells, which shows that GFP-Yif1 is degraded in the vacuole (Figure 1B).

To confirm the involvement of TOR signaling in the routing of GFP-Yif1 to the vacuole upon AA starvation, we examined the localization of GFP-Yif1 upon TOR depletion. Yeast have two *TOR* gene paralogs, *TOR1* and *TOR2* (Wullschleger et al., 2006), and the deletion of *TOR1* alone does not induce GFP-Yif1 delivery to the vacuole (Figure S1B). However, upon the depletion of both *TOR* genes (i.e., using a *tor1*Δ *GAL-TOR2* strain grown on glucose-containing medium), GFP-Yif1 was directed to the vacuole even under normal growth conditions (i.e., without AA starvation or TOR inhibition; Figure S1C). Thus, our results demonstrate that TOR repression results in GFP-Yif1 redistribution and degradation.

Additional *trans* Golgi Proteins Are Targeted to the Vacuole upon AA Starvation

Since the localization of other *trans* Golgi proteins (e.g., Kex2-GFP and GFP-Btn1) is altered in yeast Batten disease models (Kama et al., 2007, 2011), we examined whether these proteins are also directed to the vacuole upon AA starvation/TOR inhibition. We found that GFP-tagged Btn1, Tlg2 (a Golgi-endosome t-SNARE), and Kex2 (a furin-like protease) were targeted to the vacuole upon AA starvation (Figure S2A), implying that redistribution of proteins of the biosynthetic route (e.g., Golgi-endosome proteins) is not restricted to GFP-Yif1. In contrast, other GFP-tagged Golgi-endosome proteins, e.g., GFP-Sed5, Vps10-GFP, and GFP-Tlg1, as well as GFP-Snc1 (an endocytic/exocytic v-SNARE), did not reach the vacuole upon AA starvation (Figure S2B). Thus, this phenomenon is limited to a subset of *trans* Golgi proteins.

Golgi Proteins Reach the Vacuole via the VPS Pathway and Not by Autophagy

Autophagy is the major degradation route regulated by TOR signaling upon starvation. However, when we examined GFP-Yif1 localization in autophagy-deficient strains (e.g., *atg1Δ* or *atg8Δ* cells) upon starvation, we did not observe a block in its transfer to the vacuole (Figure S3A). Thus, autophagy is not involved in the routing of *trans* Golgi proteins to the vacuole.

Apart from autophagy, vacuolar proteins like carboxypeptidase 1 (Cps1) are routed from the Golgi to the vacuole via the MVB-VPS pathway (Henne et al., 2011; Hurley, 2008). To examine whether protein delivery to the vacuole upon starvation/rapamycin treatment necessitates the VPS pathway, we examined the localization of GFP-Yif1 in deletion mutants in which the pathway is blocked. Upon AA starvation, GFP-Yif1 did not reach the vacuole but accumulated in an enlarged prevacuolar class E-type (endosomal) compartment (Henne et al., 2011; Hurley, 2008) and on the vacuolar membrane (which co-label with the endosome/vacuole dye FM4-64) in an early-stage MVB mutant (e.g., *vps27Δ* cells; Figure 1C). The retention of GFP-Yif1 to the class E compartment during AA starvation was also observed in *doa4Δ* cells, which are defective in late-stage MVB formation (Figure 1C). Overall, GFP-Yif1 was not directed to the vacuole in mutants of ESCRT-0, -I, -II, and -III (Figure S3B), which clearly indicates involvement of the MVB-VPS pathway in the routing of Golgi proteins to the vacuole upon starvation.

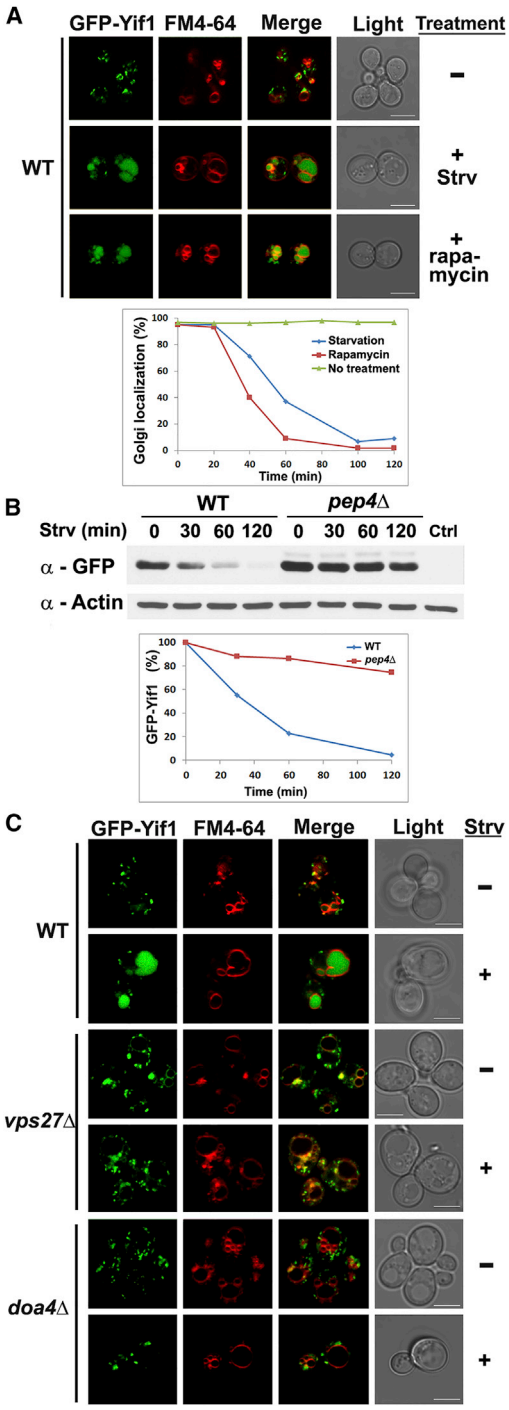

Figure 1. GFP-Yif1 Is Degraded in the Vacuole upon Starvation or Rapamycin Treatment

(A) GFP-Yif1 is targeted to the vacuole upon AA starvation or rapamycin treatment. WT cells expressing GFP-Yif1 were left untreated or either starved for AAs or treated with rapamycin, prior to labeling with FM4-64. Upper panel: images of representative cells. Lower panel: graph of the percentage of cells having GFP-Yif1 localized to the Golgi/early-endosome (i.e., small puncta) at various times after treatment (0–120 min).

(B) GFP-Yif1 is degraded in the vacuole upon AA starvation. WT and *pep4*Δ cells expressing GFP-Yif1 were treated as in (A) (but without FM4-64 labeling). Upper panel: western of cells lysed and immunodetected with anti-GFP (i.e., to detect Yif1) or -actin antibodies (i.e., as loading control). Lower panel: bands from the upper panel were quantified and graphed.

(C) GFP-Yif1 is directed to the vacuole via the VPS pathway. WT, *vps27Δ*, and *doa4Δ* cells expressing GFP-Yif1 were untreated (−) or starved (+) and labeled with FM4-64. GFP-Yif1 did not reach the vacuole upon AA starvation in ~100% of *vps27Δ* or *doa4Δ* cells.

The E2 Conjugase Ubc4 Is Involved in GFP-Yif1 Routing to the Vacuole

As ubiquitination is necessary for directing membrane proteins from the biosynthetic and endocytic routes to the lysosome/vacuole (Piper and Luzio, 2007), we examined the effect of deletions in *UBC4* and *UBC5* upon GFP-Yif1 localization during AA starvation. Ubc4 and Ubc5 are homologous E2 ubiquitin conjugases that mediate the selective degradation of short-lived/damaged proteins and are involved in cellular stress responses (Seufert and Jentsch, 1990). Additionally, Ubc4 is required for the ubiquitination and sorting of Cps1 to the MVB (Reggiori and Pelham, 2002). We found that while GFP-Yif1 is directed to the vacuole upon AA starvation in *ubc5Δ* cells, this was not observed in *ubc4Δ* cells (Figure 2A). Thus, Ubc4 function is necessary for Golgi protein routing to the vacuole.

The E3 Ligase Tul1 Is Necessary for GFP-Yif1 Delivery to the Vacuole

A Golgi-endosome protein that is not directed to the vacuole upon AA starvation or rapamycin treatment is the Tlg1 t-SNARE (Figure S2B), which is palmitoylated by the Swf1 palmitoyltransferase (Valdez-Taubas and Pelham, 2005). Yet, Tlg1 reaches the vacuole in *swf1Δ* cells, as does an unpalmitoylated form of Tlg1 (Tlg1M7) in WT cells. Unpalmitoylated Tlg1 is ubiquitinated by the Tul1 E3 ligase, in conjunction with Ubc4, and it was proposed that palmitoylation blocked Tlg1 ubiquitination by preventing exposed acidic residues from being recognized by Tul1 (Valdez-Taubas and Pelham, 2005).

Because the vacuolar localization of unpalmitoylated Tlg1 is reminiscent of our findings made with other *trans* Golgi proteins, and as this involves Ubc4, we examined the effect of AA starvation on the localization of unpalmitoylated GFP-Tlg1. In contrast to the results of Pelham and colleagues, we found that unpalmitoylated Tlg1 (i.e., either GFP-Tlg1 expressed in *swf1Δ* cells or GFP-Tlg1M7 expressed in WT cells) was not significantly directed to the vacuole under nutrient-rich conditions. In contrast, however, both GFP-Tlg1 in *swf1Δ* cells and GFP-Tlg1M7 in WT cells were routed to the vacuole upon AA starvation (Figure 2B). This was identical to that observed for GFP-Yif1, GFP-Tlg2, or GFP-Btn1 in WT cells (Figures 1A and S2A) but unlike palmitoylated GFP-Tlg1, which remained in the Golgi (Figure S2B). Correspondingly, we found that unpalmitoylated (and non-GFP-tagged) Tlg1 (e.g., Myc-Tlg1 in *swf1Δ* cells) is degraded only upon AA starvation (Figure 3B). These results strongly suggest that the earlier work on Tlg1 (Valdez-Taubas and Pelham, 2005) may have been performed under non-optimal growth conditions (i.e., using overgrown/stressed cultures) in which a starvation effect (as shown in Figure S1A) was induced.

As GFP-Tlg1 is ubiquitinated by Ubc4 (Valdez-Taubas and Pelham, 2005) and its unpalmitoylated form localized to the

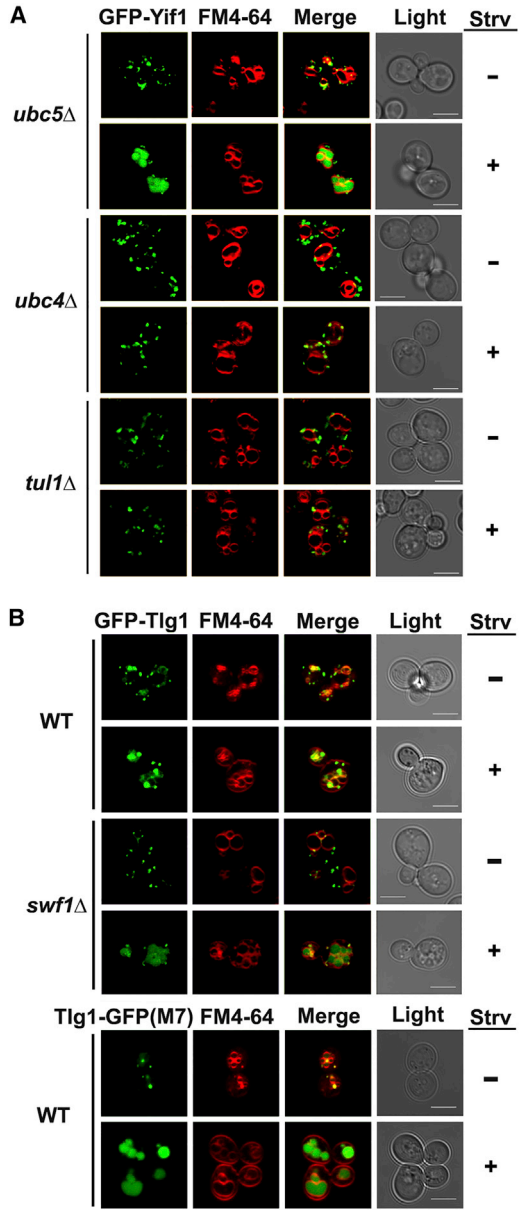

Figure 2. Ubc4 and Tul1 Mediate the Localization of GQC Substrates upon Starvation

(A) GFP-Yif1 targeting to the vacuole upon starvation is blocked in *ubc4*Δ and *tul1*Δ cells. *ubc4Δ*, *ubc5Δ*, and *tul1Δ* cells expressing GFP-Yif1 were either maintained on synthetic rich medium (–) or shifted to AA starvation medium (+), and then labeled with FM4-64. Representative images are shown; GFP-Yif1 labeled the vacuole in ~100% of *ubc5Δ* cells upon AA starvation, but not in *ubc4Δ* (~10%) or *tul1*Δ cells (~0%).

(B) Unpalmitoylated Tlg1, a GQC substrate, is targeted to the vacuole upon AA starvation. WT cells and *swf1*Δ cells expressing GFP-Tlg1 (upper panels) or WT cells expressing GFP-Tlg1(M7) (lower panels) were either maintained on nutrient-rich medium (–) or shifted to AA starvation medium (+) and then labeled with FM4-64. Unpalmitoylated Tlg1 (i.e., GFP-Tlg1 in *swf1*Δ cells and Tlg1(M7) in WT cells), but not palmitoylated Tlg1, is routed to the vacuole upon starvation in ~100% of cells.

vacuole upon AA starvation (Figure 2B), we tested the involvement of Tul1 in the routing of *trans* Golgi proteins. Indeed, GFP-Yif1 delivery to the vacuole did not occur in a *tul1Δ* deletion strain upon AA starvation (Figure 2A). Correspondingly, the deletion of either *UBC4* or *TUL1* protected GFP-Yif1 from undergoing degradation (Figure 3A, top panel). Yet, when *TUL*1 was overexpressed, GFP-Yif1 remained essentially localized to the Golgi (Figure S4D). Thus, Yif1 localization to the vacuole upon starvation appears to involve ubiquitination via Ubc4 and Tul1.

GQC Substrates Are Ubiquitinated and Targeted to the Vacuole upon AA Starvation

As our results indicate that Ubc4 and Tul1 ubiquitinate Yif1, we verified this by western analysis using anti-ubiquitin antibodies (Figure 3A, second panel). Indeed, we found that Yif1 is ubiquitinated in WT cells, and this is dependent on both *UBC4* and *TUL1*, since ubiquitinated (and higher-molecular-mass) GFP-Yif1 was hardly detected upon their deletion (Figure 3A, second and third panels). Moreover, upon the deletion of *VPS27* (which prevents protein entry into the MVB and results in the accumulation of ubiquitinated cargo), we observed an accumulation of ubiquitinated GFP-Yif1 and no release of free GFP (Figure 3A). Thus, Yif1 behaves like other biosynthetic cargo proteins destined to reach the vacuole (e.g., Cps1). Interestingly, we observed that GFP-Yif1 is ubiquitinated during growth on nutrient-rich medium in WT cells and that the ubiquitinated bands disappeared upon AA starvation (Figure 3A). Together, these results support a model by which Golgi-localized GFP-Yif1 is ubiquitinated by Ubc4 and Tul1 during normal growth but becomes directed to the vacuole via the VPS pathway upon starvation/TOR inactivation. This would also imply that upregulation of the VPS pathway (and not ubiquitination per se) directs Golgi proteins to the vacuole.

Importantly, Ubc4 and Tul1 have been characterized as GQC components that ubiquitinate membrane proteins that are either damaged or in their non-native conformation, this being typified by TMDs containing polar residues (e.g., unpalmitoylated Tlg1) exposed to the lipid bilayer (Hettema et al., 2004; Reggiori and Pelham, 2002; Valdez-Taubas and Pelham, 2005). Thus, our observations suggest that TOR inactivation re-localizes GQC substrates from the Golgi to the vacuole. To verify this using a non-GFP-tagged substrate, we examined whether unpalmitoylated Myc-Tlg1, which was previously characterized as a GQC substrate that undergoes ubiquitination (Valdez-Taubas and Pelham, 2005), exhibits higher-molecular-mass (i.e., ubiquitinated) forms prior to AA starvation. Indeed, higher-molecular-mass forms of Myc-Tlg1 in *swf1Δ* cells were detected under nutrient-rich conditions. However, these forms disappeared along with non-ubiquitinated Myc-Tlg1 only upon AA starvation (Figure 3B). Thus, unpalmitoylated Tlg1 is recognized as a GQC substrate, but is degraded only upon starvation. This result implies that GFP-Yif1 is also recognized by the GQC system as a malfolded protein, even if it is functional and complements *yif1Δ* deletion strains under normal growth conditions. Importantly, Yif1 is not degraded upon AA starvation when conjugated to a smaller epitope tag (e.g., N-terminal hemagglutinin [HA] tag; Figures 3C–3E and S4A) or conjugated to a C-terminal HA tag from its native promoter (Figure S4A). This implies that

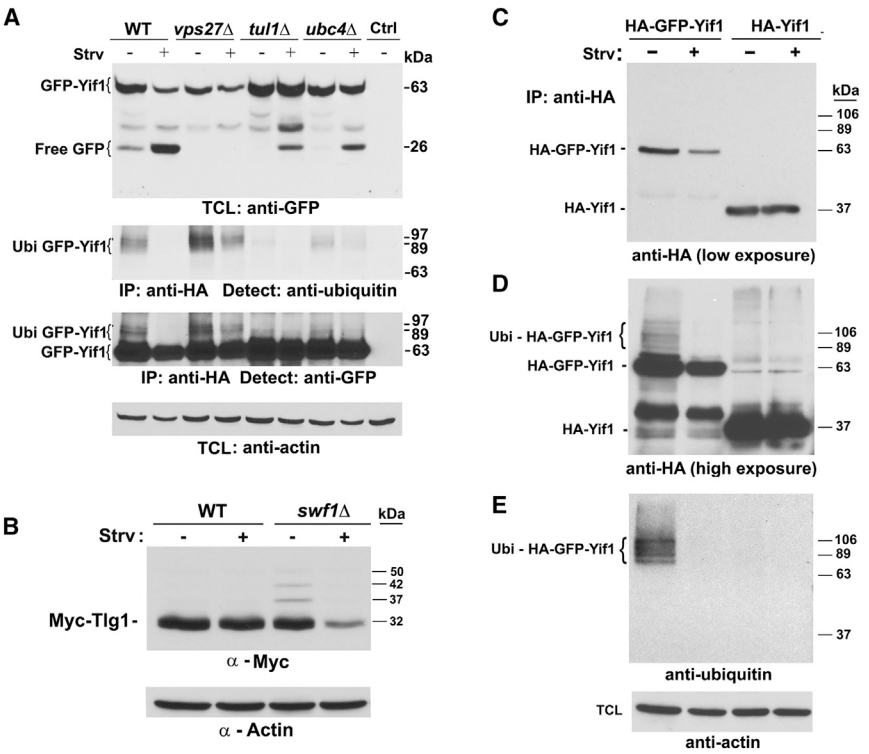

Figure 3. GFP-Yif1 Degradation upon Starvation Reveals a Link between GQC and TOR Signaling

(A) Ubc4 and Tul1 act upstream to Vps27 to mediate GFP-Yif1 ubiquitination and degradation. WT, *vps27Δ*, *ubc4Δ*, and *tul1Δ* cells expressing HA-GFP-Yif1 were maintained on synthetic-rich medium (–) or shifted to AA starvation medium for 2 hr (+) and processed for immunoprecipitation (IP). HA-GFP-Yif1 was detected in lysates derived from WT, *vps27Δ*, *ubc4Δ*, and *tul1Δ* cells (as labeled) using anti-GFP antibodies to examine degradation (i.e., release of free GFP; top panel) and anti-actin (i.e., as a loading control; bottom panel). Aliquots of the lysates were used in IPs with anti-HA-conjugated Sepharose beads and detected in westerns using anti-ubiquitin and anti-GFP antibodies to examine GFP-Yif1 ubiquitination directly (second panel) and indirectly (i.e., high-molecular-mass ubiquitinated forms; third panel), respectively. Molecular mass is in kDa. Bands corresponding to ubiquitin-labeled GFP-Yif1 ("Ubi GFP-Yif1"), GFP-Yif1 ("GFP-Yif1"), and released GFP ("Free GFP") are marked accordingly. Actin was detected as a loading control.

(B) Unpalmitoylated Tlg1 is degraded only upon AA starvation. WT and *swf1Δ* cells expressing Myc-Tlg1 were treated as in (A), and Tlg1 was detected in the lysates by western blotting using anti-Myc antibodies. Actin was detected as a loading control.

(C–E) HA-GFP-Yif1, but not HA-Yif1, is a GQC substrate. WT yeast expressing HA-GFP-Yif1 or HA-Yif1 were treated and processed for IP as described in (A). Aliquots of the lysates were subjected to IP with anti-HA-conjugated Sepharose beads and proteins detected in westerns using anti-HA antibodies (C, low-exposure blot; D, high-exposure blot to detect high-molecular-mass [i.e., ubiquitinated] forms) or anti-ubiquitin antibodies (E) to detect ubiquitinated HA-tagged Yif1 substrates directly. Lower panel: aliquots of lysates were detected for actin as a loading control. Unlike HA-GFP-Yif1, HA-Yif1 did not undergo ubiquitination or degradation upon starvation.

GFP tagging of Golgi proteins may cause them to be recognized by the GQC machinery as aberrant/non-native proteins.

We examined potential ubiquitination sites on the cytoplasmic tail of Yif1 by mutational analysis. Mutation of lysine-93 to arginine (e.g., GFP-Yif1^{K93R}) caused the retention of GFP-Yif1^{K93R} to the Golgi upon AA starvation (Figure S4B) and thereby reduced its degradation (Figure S4C). Thus, Yif1 and not the GFP moiety is the likely substrate for Ubc4-Tul1. Since GFP-Yif1 was ubiquitinated even under normal growth conditions (Figure 3A), we examined whether HA-tagged Yif1 is ubiquitinated. Interestingly, we could not detect the ubiquitination of HA-Yif1 using anti-ubiquitin antibodies under nutrient-rich or AA starvation conditions (Figure 3E). In contrast, ubiquitinated HA-GFP-Yif1 was clearly detectable under nutrient-rich conditions (Figures 3D and 3E), but not under starvation conditions, when it is directed to the vacuole and degraded. Thus GFP-Yif1, but not HA-tagged Yif1, is a GQC substrate. This finding is in full agreement with the idea that GQC recognizes only malfolded/damaged proteins.

The Trafficking of Golgi and PM Proteins to the Vacuole Is Upregulated upon AA Starvation and Is Independent of Ist1

PM permeases (e.g., Fur4) become ubiquitinated and reach the vacuole via the VPS pathway upon starvation (Lauwers et al., 2010). We verified that Fur4-GFP localized to the vacuolar lumen in WT cells upon AA starvation, in contrast to its primary localization to the PM/endosomes under nutrient-rich conditions (Figure S5A). Moreover, Fur4-GFP localized to large class E puncta in cells lacking *VPS27* upon AA starvation and did not access the vacuolar lumen (Figure S5A). Thus, Fur4-GFP behaves similarly to GFP-Yif1 upon AA starvation (i.e., relocalization to the vacuole and degradation). Work by Babst and colleagues revealed that AA starvation induces upregulation of the VPS pathway, resulting in permease transport to the vacuole. They proposed that VPS upregulation occurs via proteasome-mediated degradation of Ist1, a putative negative regulator of ESCRT-III (Jones et al., 2012). To check if Ist1 regulates the relocalization of GQC substrates to the vacuole, we examined the localization of GFP-Yif1 in *ist1Δ* cells. Interestingly, the deletion of *IST1* did not affect either GFP-Yif1 or Fur4-GFP localization to the vacuole under normal nutrient-rich conditions or upon AA starvation (Figure S5B). This result suggests that Ist1 function does not necessarily play a role in upregulation of the VPS pathway with respect to the trafficking of endocytosed or biosynthetic pathway membrane proteins.

A Link between the Proteasome and GQC-Mediated Protein Trafficking to the Vacuole

As the deletion of *IST1* had no effect upon either GFP-Yif1 or Fur4-GFP trafficking, we suspected that degradation of another

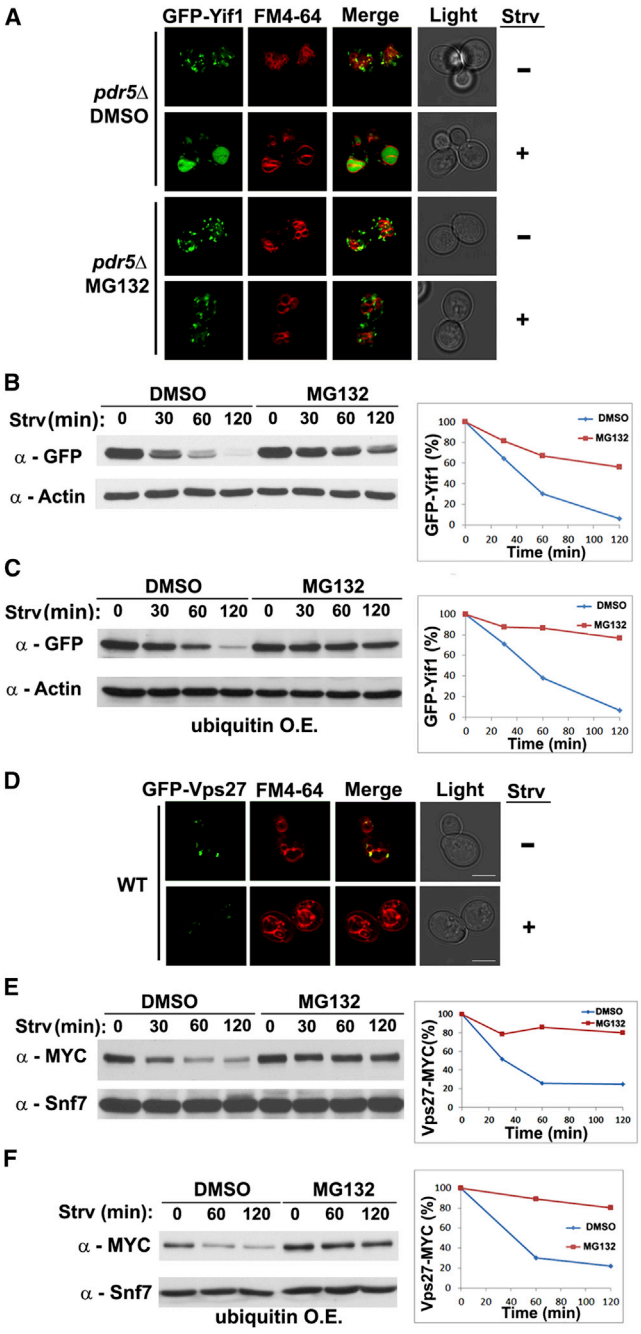

Figure 4. Proteasome Inhibition by MG132 Blocks Vps27 Degradation and GQC

(A) MG132 treatment blocks GFP-Yif1 targeting to the vacuole. *pdr5Δ* cells expressing GFP-Yif1 were pre-treated either with MG132 (50 μM; "MG132") or DMSO (as control; "DMSO") for 15 min prior to shifting them to AA starvation medium or maintaining them on synthetic-rich medium for 1.5 hr (in the presence of added DMSO or MG132). Cells were then labeled with FM4-64. Upon AA starvation in the presence of MG132, GFP-Yif1 was Golgi-localized in ~87% of cells, but localized to the vacuole in ~100% of control cells (i.e., without MG132 treatment).

(B and C) GFP-Yif1 degradation upon starvation is inhibited by MG132. *pdr5Δ* cells expressing GFP-Yif1 alone (B) or the same cells also overexpressing ubiquitin from a multicopy plasmid (C) were treated for 2 hr with or without MG132, lysed, and subjected to western analysis (top panels) using anti-GFP antibodies to detect GFP-Yif1 and anti-actin antibodies (as loading control). Lower panel: bands from the anti-GFP panel were quantified, normalized, and graphed as the percentage of GFP-Yif1 remaining from time 0.

(D) GFP-Vps27 disappears upon starvation. WT cells expressing GFP-Vps27 from a multi-copy plasmid were maintained on synthetic-rich medium (–) or shifted to AA starvation medium (+) for 2 hr.

(E and F) Vps27 is degraded upon starvation in a proteasome-dependent manner. *pdr5Δ* cells expressing *VPS27-MYC* from its genomic locus (E) or the same cells also overexpressing ubiquitin from a multicopy plasmid (F) were treated with or without MG132 for 15 min and then shifted to AA starvation medium for 0–120 min. Cells were processed for western analysis (upper panels) using anti-myc antibodies to detect Vps27-Myc and anti-Snf7 (as loading control). Lower panel: bands from the anti-myc panel were quantified, normalized, and graphed as the percentage of Vps27-myc present as a function of time upon AA starvation. MG132 treatment inhibits both the degradation of GFP-Yif1 in the vacuole and the degradation of Vps27 by the proteasome.

factor might be involved in VPS pathway upregulation upon AA starvation. Therefore, we inhibited proteasome-mediated protein degradation using the MG132 proteasome inhibitor in yeast lacking the Pdr5 multidrug transporter (i.e., *pdr5Δ* cells). These cells are more sensitive to MG132 and thus are commonly used in proteasome inhibition assays. Importantly, GFP-Yif1 was not directed to the vacuole upon AA starvation in MG132-treated *pdr5Δ* cells (Figure 4A) and was not degraded in the vacuole to the same extent as untreated cells after 2 hr (e.g., 40% versus 95% degradation, respectively; Figure 4B). Similar results were obtained even when ubiquitin was overexpressed (Figure 4C), which eliminates the concern that ubiquitin depletion might block GFP-Yif1 delivery to the vacuole in the presence of proteasome inhibitor. Thus, proteasome-mediated protein degradation facilitates VPS pathway upregulation upon AA starvation.

We initially examined the degradation of proteins involved in the first stage in the MVB sorting, namely ESCRT-0 (e.g., Vps27 and Hse1), which binds to and clusters ubiquitinated proteins destined for MVB entry (Bilodeau et al., 2002; Hirano et al., 2006; Wollert and Hurley, 2010) and recruits clathrin and deubiquitinating enzymes (Henne et al., 2011; Hurley, 2008). Importantly, we observed that HA-tagged Vps27 was almost completely degraded after only 1 hr of AA starvation, while Hse1 was substantially degraded (e.g., 85% and 59% degraded; Figure S6A). In agreement with the western analysis, we also observed that GFP-Vps27 disappeared from late endosomes in response to AA starvation in WT cells (Figure 4D). Moreover, we did not detect any accumulation of GFP in the vacuole, implying that its degradation is mediated by the proteasome. Therefore, we monitored HA-Vps27 levels in *pdr5Δ* cells upon AA starvation in the presence of MG-132 and observed a substantial block in HA-Vps27 degradation (e.g., <20% degradation in the presence of MG132 and >80% in its absence; Figure 4E). A similar block in HA-Vps27 degradation was observed even when ubiquitin was overexpressed, indicating that the loss in degradation is not due to ubiquitin depletion (Figure 4F). Thus, proteasome-mediated degradation of ESCRT-0 components (Vps27 and Hse1) and VPS pathway upregulation coincide.

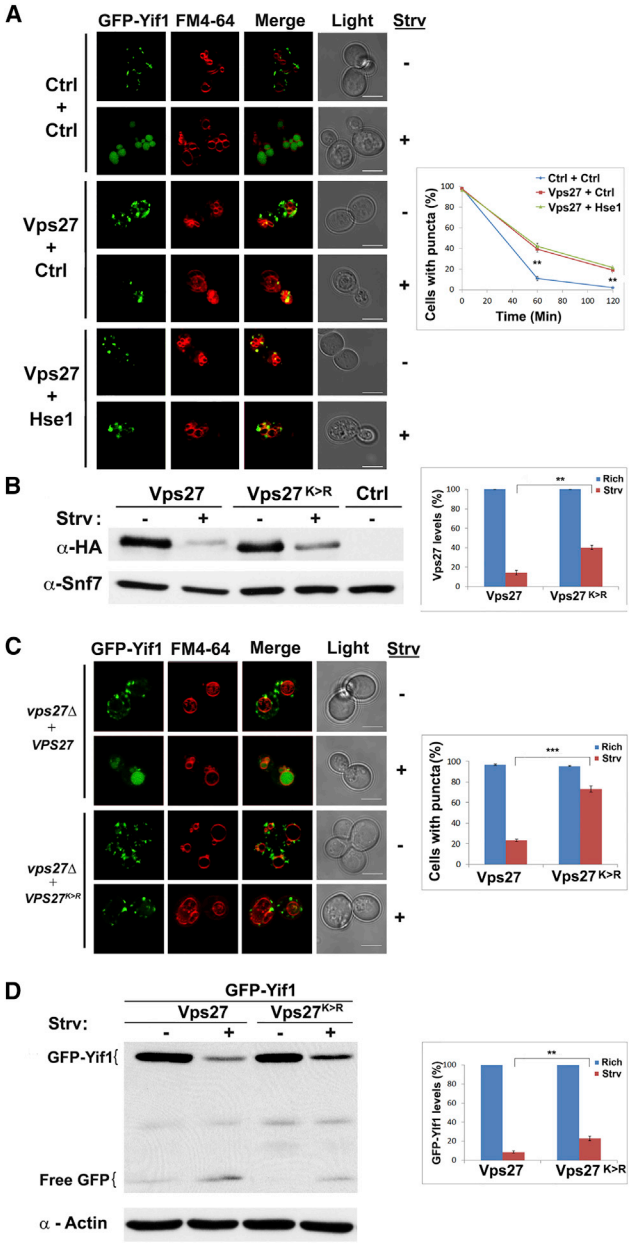

Figure 5. A Lysine-to-Arginine Substitution Mutant of Vps27 Represses the Delivery of GFP-Yif1 to the Vacuole upon AA Starvation

(A) Overexpression of HA-Vps27 inhibits GFP-Yif1 delivery to the vacuole upon starvation. WT cells expressing GFP-Yif1 were transformed with control plasmids (Ctrl + Ctrl) and either multi-copy plasmids expressing HA-Vps27 (Vps27 + Ctrl) or HA-Vps27 and Myc-Hse1 (Vps27 + Hse1). Cells were maintained in selective rich medium or shifted for AA starvation for 1.5 hr prior to labeling with FM4-64. Cells were examined by confocal microscopy (left panel), and those having GFP-Yif1 localization to Golgi-endosome puncta before and after starvation were scored (as % of cells; right panel). After starvation, GFP-Yif1 localized to Golgi puncta in 2% ± 0.6% of control cells but showed 19% ± 2.1% and 21.7% ± 1.8% Golgi localization in cells expressing HA-Vps27 alone or HA-Vps27 and Myc-Hse1, respectively (**$p < 0.01$). Representative pictures of Golgi localization after AA starvation are shown.

(B) Vps27 lacking lysine residues is more stable upon AA starvation. *vps27*Δ (BY4742; *MET*$^+$) cells expressing HA-Vps27 or HA-Vps27$^{K>R}$ (which bears K»R substitutions) under a methionine starvation-inducible promoter (*MET25*) were either maintained in selective medium lacking methionine or shifted to AA starvation medium for 2 hr before processing for western analysis. Left panel: proteins were detected in blots using anti-HA antibodies to detect Vps27 proteins or anti-Snf7 antibodies (as loading control). Right panel: bands were quantified using GelQuantNet and graphed as the amount (in %) of the treated sample relative to the untreated sample. The levels of HA-Vps27 and HA-Vps27$^{K>R}$ after AA starvation were 15.1% ± 2.4% and 42.3% ± 2.2% of initial levels, respectively (**$p < 0.01$).

(C) Expression of HA-Vps27$^{K>R}$ inhibits GFP-Yif1 delivery to the vacuole upon starvation. The same cells as in (B) expressing GFP-Yif1 were maintained in selective rich medium or shifted to AA starvation medium for 1.5 hr. Cells were labeled with FM4-64 and visualized by confocal microscopy, and those having GFP-Yif1 localization to Golgi-endosome puncta before and after starvation were scored (as % of cells; right panel; 73.0% ± 3.1% of HA-Vps27$^{K>R}$ cells versus 23.3% ± 1.2% in HA-Vps27 cells had dot-like puncta only; ***$p < 0.001$).

(D) GFP-Yif1 degradation is repressed by HA-Vps27$^{K>R}$. The same cells as in (C), along with control cells expressing HA-Vps27 but lacking GFP-Yif1, were maintained in selective rich medium or shifted to AA starvation medium for 2 hr and processed for western analysis. Left panel: proteins were detected in immunoblots using anti-GFP antibodies to detect GFP-Yif1 or anti-actin antibodies (as loading control). Right panel: bands were quantified using GelQuantNet and graphed as the amount (in %) of the treated sample relative to the untreated sample. The levels of GFP-Yif1 in cells expressing HA-Vps27 or HA-Vps27$^{K>R}$ after AA starvation were 8.7% ± 1.5% and 22.9% ± 2.3%, respectively, of initial levels. Degradation products of GFP-Yif1 (i.e., free GFP) were observed in cells overexpressing HA-Vps27, while lesser signals were observed in cells overexpressing HA-Vps27$^{K>R}$ (**$p < 0.01$).

If Vps27 degradation is required for GFP-Yif1 delivery to the vacuole, we hypothesized that the overexpression of Vps27 might disrupt this process. Indeed, HA-Vps27 overexpression from a multicopy plasmid inhibited GFP-Yif1 targeting to the vacuole (Figure 5A). Moreover, as protein degradation by the proteasome involves ubiquitination and lysines are the most common site for modification, we examined whether Vps27 in which all lysines were mutated to arginines (Vps27$^{K>R}$; Stringer and Piper, 2011) is stabilized upon AA starvation. Indeed, 3-fold more HA-Vps27$^{K>R}$ was present (in comparison to HA-Vps27) after AA starvation (Figure 5B). We then tested whether HA-Vps27$^{K>R}$ expression could inhibit GFP-Yif1 relocalization and degradation. HA-Vps27$^{K>R}$ expressed from a single-copy plasmid in *vps27*Δ cells was found to suppress GFP-Yif1 delivery to the vacuole upon AA starvation, as seen by fluorescence microscopy (Figure 5C). Similar results were obtained by HA-Vps27$^{K>R}$ expression from a multicopy plasmid (data not shown). Consequently, upon AA starvation, ~3-fold more GFP-Yif1 was observed in lysates derived from cells expressing HA-Vps27$^{K>R}$ than from cells expressing HA-Vps27 (Figure 5D), and less free GFP was observed in cells expressing HA-Vps27$^{K>R}$. Thus, a more stable version of Vps27 (e.g., HA-Vps27$^{K>R}$) suppresses GQC transfer to the vacuole.

Finally, we verified that HA-Vps27$^{K>R}$ functions similar to HA-Vps27 under starvation conditions, as previously shown using Cps1 under normal growth conditions (Stringer and Piper, 2011). We observed efficient GFP-Cps1 sorting to the vacuole under both starvation and non-starvation conditions in cells expressing HA-Vps27$^{K>R}$ (Figure S6E). Overall, these results suggest that proteasome-mediated degradation of the Vps27 ESCRT-0 component facilitates GQC. In contrast, Vps23, a

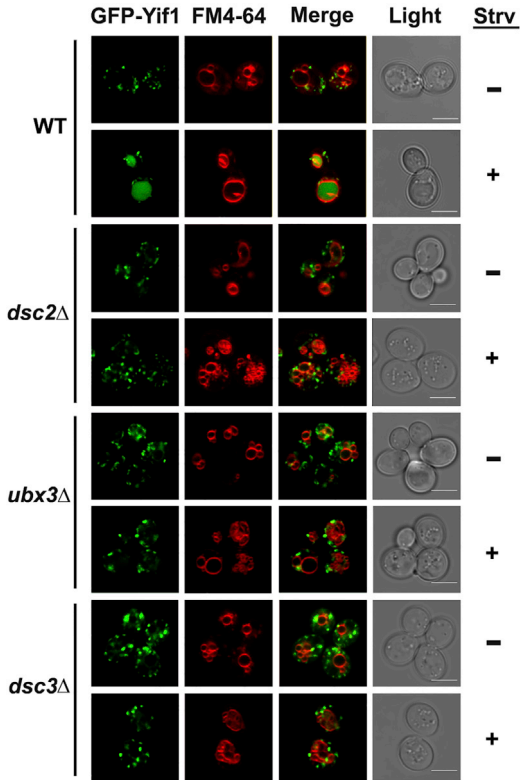

Figure 6. The DSC Complex Mediates GQC

WT, *dsc2*Δ, *dsc3*Δ, and *ubx3*Δ cells expressing GFP-Yif1 were maintained in selective rich medium or shifted to AA starvation medium prior to labeling with FM4-64. Deletions in *DSC2, DCS3,* and *UBX3* blocked GFP-Yif1 targeting to the vacuole upon AA starvation in ~100% of cells.

component of the downstream ESCRT-I complex that interacts with the same ubiquitinated residues as ESCRT-0, is stable upon AA starvation (Bilodeau et al., 2003; Katzmann et al., 2003) (Figure S6B). Likewise, Snf7, a component of ESCRT-III was also stable in these assays (Figures 4E, 4F, 5B, and S6B). This indicates that TOR signaling might specifically regulate the levels of ESCRT-0.

While Vps27 and other ESCRT components undergo ubiquitination, no change in their functionality was observed (Shields and Piper, 2011; Stringer and Piper, 2011). However, those experiments were performed under normal growth conditions and not upon TOR attenuation. Thus, Vps27 and the other ESCRT components may not have been targeted for degradation. Our results implicate rapid proteasome-mediated degradation of Vps27 (and not Ist1) upon AA starvation as a means to upregulate the VPS pathway upon nutrient-limitation. This implies that GQC substrates might co-localize with Vps27/ESCRT-0 prior to AA starvation. Indeed, GFP-Yif1 co-localizes somewhat with both early and late endosomes (i.e., small and large puncta, respectively) in WT yeast labeled briefly with FM4-64 (Figure S6C) or expressing red fluorescent protein (RFP)-Vps27, respectively (Figure S6D). However, after a short (e.g., 40-min) period of AA starvation, GFP-Yif1 localized primarily with RFP-Vps27-labeled late endosomes. And after 2 hr of starvation, no RFP-Vps27 could be detected and GFP-Yif1 was localized to the vacuole (Figure S6D). Thus, GQC substrates access endosomes and perhaps transiently interact with ESCRT components prior to VPS upregulation upon starvation.

Genome-wide Screening for Additional GQC Components Identifies the DSC Complex

To identify other components involved in the vacuolar localization of Golgi proteins upon AA starvation, we performed a non-biased visual screen in which we co-expressed GFP-Yif1 and a vacuolar marker (e.g., mCherry-Vph1) in a viable deletion strain collection (~5,200 strains) and a hypomorphic allele collection (~1,100 strains). We screened for strains in which GFP-Yif1 did not localize to the vacuole in response to rapamycin treatment (which recapitulates the effect of AA starvation) or was directed to the vacuole under nutrient-rich growth conditions (Table S1). Deletion strains lacking *UBC4* or *TUL1* served as positive internal controls. Consistent with our previous results, we identified deletions in genes involved in endosomal protein trafficking (e.g., ESCRT-0–III), cellular starvation responses (e.g., *FPR1*, which encodes a rapamycin-binding protein), and AA homeostasis (e.g., *LYS14*). However, we did not identify components involved endosomal protein retrieval (e.g., retromer), as they did not cause significant GFP-Yif1 localization to the vacuole under normal growth conditions. We did observe that GFP-Yif1 was not fully localized to the vacuole upon rapamycin treatment in the deletion strain of *RPN4*, which encodes a transcription factor that regulates proteasome genes (Zhang et al., 2013). This finding supports our results obtained using MG132 (Figure 4A).

Importantly, we identified orthologs of the *S. pombe* DSC complex (e.g., *DSC3* and *UBX3*) as being necessary for GFP-Yif1 delivery to the vacuole upon rapamycin treatment (Table S1). The fission yeast complex (Dsc1-3 and Ucp10) is proposed to facilitate the ubiquitination and proteasome-mediated cleavage of membrane-bound SREBP (Stewart et al., 2011) and is conserved in *S. cerevisiae* (Ryan et al., 2012). Yet, since SREBPs are lacking in budding yeast, the function of this complex is not clear. Although Tul1 is the Dsc1 ortholog (Ryan et al., 2012) and quantitative proteomics using SILAC identified >50 substrates whose expression is altered in *tul1Δ* cells, no common connection has been surmised (Tong et al., 2014). We did not identify *DSC2* in our screen, since its deletion was absent from the library. Hence, we manually tested the localization of GFP-Yif1 in a *dsc2Δ* deletion strain, along with *ubxΔ3* and *dsc3Δ* deletion mutants, upon AA starvation. GFP-Yif1 did not localize to the vacuole in any of these mutants (Figure 6); thus, the intact DSC complex is essential for GQC.

DISCUSSION

Studies using yeast as a model for Batten disease showed that specific *trans* Golgi proteins are routed to the endolysosomal pathway for inactivation, indicating that altered protein trafficking might be connected to disease pathology (Kama et al., 2011). The same subset of GFP-tagged Golgi/early endosome proteins (e.g., Yif1, Tlg2, Kex2, and Btn1) is rapidly delivered to the vacuole in WT cells upon TOR inactivation (e.g., upon rapamycin treatment, AA starvation, or TOR shut-off; Figures 1A, S1C, and S2A). This

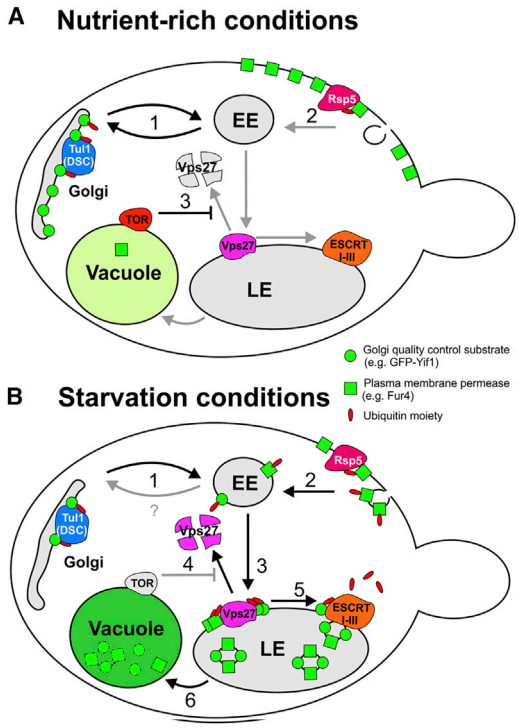

Figure 7. TOR-Regulated Golgi Quality Control

Mono-ubiquitinated Golgi quality control substrates (GQC; e.g., GFP-Yif1) and plasma membrane (PM) permeases (e.g., Fur4-GFP) are sorted to the vacuole upon TOR inactivation (i.e., AA starvation) via the MVB-VPS pathway in a process that requires the degradation of ESCRT-0 components (e.g., Vps27).

(A) Nutrient-rich conditions (i.e., TOR active): (1) GQC substrates (e.g., GFP-Yif1; green circles) are ubiquitinated by the Tul1-DSC complex but reside at steady-state in the Golgi due to retrieval from early endosomes (EE); (2) PM permeases (e.g., Fur4-GFP; green squares) reside on the PM (although a small fraction may be delivered to the vacuole for degradation); and (3) Tor signaling blocks proteasome-mediated degradation of Vps27, an ESCRT-0 component that resides on the late endosome (LE).

(B) Starvation conditions (i.e., TOR inactive): (1) ubiquitinated GQC substrates are not retrieved and thus sort to the EE; (2) Fur4-GFP is ubiquitinated by Rsp5 and undergoes endocytosis and delivery to the EE; (3) Vps27 binds to and clusters ubiquitinated substrates that arrive from the Golgi and PM via the EE; (4) as a consequence of TOR repression, Vps27 becomes targeted for degradation in a proteasome-dependent fashion; (5) the ubiquitin moieties of the cargo proteins are now free to interact with the downstream ESCRT machinery (e.g., ESCRT-I-III) and enter intralumenal vesicles upon deubiquitination; and (6) intralumenal vesicles are degraded upon LE/MVB fusion with the vacuole, leading to substrate degradation.

indicates that nutrient sensing controls the localization and degradation of Golgi proteins, similar to that described for PM-localized permeases (Jones et al., 2012). Importantly, Golgi protein targeting to the vacuole was independent of autophagy (Figure S3A) but necessitates the VPS pathway, which controls the delivery of ubiquitinated biosynthetic and endocytosed proteins to the vacuole. By using GFP-Yif1 as a model Golgi protein that is relocalized to and degraded in the vacuole upon TOR inactivation in WT cells (e.g., Figures 1, 3, 4B, 4C, 5A, 5C, 5D, S1, S3, and S4B–S4D), we found that its sorting to the vacuole was blocked in VPS pathway mutants, including all ESCRT deletion strains (Figures 1C and S3B; Table S1). Because the VPS pathway directs ubiquitinated proteins to the vacuole, we verified that GFP-Yif1 is ubiquitinated (Figure 3) and identified the E2 and E3 ubiquitination machinery (Ubc4 and Tul1, respectively) using genetic (Figure 2A; Table S1) and biochemical techniques (Figure 3A). Interestingly, GFP-Yif1 ubiquitination is constitutive (Figures 3A and 3E), but the protein is sorted to and degraded in the vacuole only upon TOR inactivation and only when VPS pathway is intact. Similar results were obtained using unpalmitoylated Tlg1 (Figure 3B). Therefore, we examined the role of TOR inactivation upon the VPS pathway and found that the ESCRT-0 components Vps27 and Hse1, but not other ESCRT-I and -III factors (e.g., Vps23 and Snf7, respectively; Figures 4E, 4F, 5B, and S6B), are degraded upon AA starvation in a proteasome-dependent manner (Figures 4D–4F, S6A, and S6D). Thus, the downregulation of GFP-Yif1 upon TOR inactivation correlates with the degradation of ESCRT-0, which normally functions in the clustering and delivery of ubiquitinated substrates to ESCRT-I. This is supported by three additional findings. First, use of a $Vps27^{K>R}$ lysine substitution mutant that is more stable than native Vps27 (Figures 5A and 5B) inhibited GFP-Yif1 redistribution and degradation upon AA starvation (Figure 5C and D). Second, use of a proteasome inhibitor (Figures 4A–4C, 4E, and 4F) or a mutation in *RPN4* (Table S1), which regulates the expression of proteasome subunits, inhibited GFP-Yif1 sorting to the vacuole and degradation. Moreover, ubiquitin overexpression did not restore GFP-Yif1 targeting to the vacuole, indicating that ubiquitin was not limiting in these experiments (Figure 4C). Third, overexpression of Vps27 partially inhibited the delivery of GFP-Yif1 to the vacuole and its degradation (Figure 5A). Therefore, VPS pathway upregulation is proteasome-dependent and is connected to the degradation of ESCRT-0.

Previous work showed that permease delivery to the vacuole is upregulated upon AA starvation and helps maintain a critical pool of free AAs for protein synthesis early in starvation, whereas autophagy is important for the supply of AAs late in starvation (i.e., after 2 hr) (Jones et al., 2012; Müller et al., 2015). While not GQC substrates, these permeases were proposed to undergo delivery to the vacuole upon starvation due to VPS pathway upregulation as a consequence of proteasome-mediated degradation of Ist1 (Jones et al., 2012). However, we could not observe any effect of an *ist1Δ* deletion upon the localization of either biosynthetic (e.g., GFP-Yif1) or endocytic (e.g., Fur4-GFP) VPS pathway substrates under normal growth conditions (Figure S5B). Rather, we propose that the proteasome-mediated degradation of ESCRT-0 (e.g., Vps27, Hse1) observed upon starvation might release clustered GQC substrates and thereby allow them to interact with downstream ESCRT-I components. Cargo clustering by ESCRT-0 has also been observed with the mammalian orthologs of Vps27 and Hse1 (e.g., Hrs and STAM) and was suggested to result from a stiff structure formed between flat clathrin and ESCRT-0 (Raiborg et al., 2006; Sachse et al., 2002). This might interfere with the subsequent binding of ESCRT-I with the ubiquitinated cargos. Hence, Raiborg et al. (2006) suggested that the exchange of Hrs (and clathrin) with the cytosolic pool might generate space for the recruitment of ESCRT-I. Correspondingly, the accelerated degradation of Hrs would facilitate the recruitment of ESCRT-I and is consistent with our model for the sorting of GQC substrates to the vacuole for degradation (see Figure 7). It is important to note that

proteasome-mediated degradation of ESCRT-0 is not comparable to a deletion of *VPS27*, since there is no initial substrate recognition by ESCRT-0 in this case. We also note that despite work showing that Vps27 is phosphorylated by the Pkh1/2 kinases to control Cps1 and PM protein trafficking to the MVB (Morvan et al., 2012), we did not identify these kinases in our genetic screen (Table S1), nor did phosphomimic or non-phosphorylated forms of Vps27 alter vacuolar sorting of GFP-Yif1 upon starvation (data not shown). Thus, Vps27 may undergo differential regulation by multiple signals that could potentially modify its ability to recognize substrates under different conditions of growth.

This study expands our knowledge regarding the GQC machinery (e.g., Ubc4 and Tul1) described by Pelham and colleagues and the vacuolar sorting and degradation of a subset of *trans* Golgi proteins. We identified Tul1 as the relevant E3 ligase for the ubiquitination of GFP-Yif1 (Figures 2A and 3A) and show that all of the components of the putative *S. cerevisiae* DSC complex are required for GQC (Figure 6; Table S1). Thus, the DSC complex mediates GQC and ubiquitinates misfolded/damaged proteins containing TMDs with polar residues exposed to the lipid bilayer (i.e., a non-native conformation), which may represent an ever-occurring fraction of the protein population (Hettema et al., 2004; Reggiori and Pelham, 2002; Valdez-Taubas and Pelham, 2005). This apparently is the case for GQC substrates like GFP-Yif1, which has an N-terminal GFP fusion, but not for HA-Yif1, which has a small N-terminal epitope fusion and is not recognized by the DSC complex (Figure 3C–3E). Thus, the DSC complex singles out specific targets that are apparently less well conformed (e.g., GFP-Yif1, GFP-Btn1, GFP-Tlg2, and GFP-Tlg1M7, in WT cells and unpalmitoylated GFP- or Myc-Tlg1 in *swf1Δ* cells). GFP tagging of these biosynthetic pathway substrates presumably mirrors a malfolded/damaged state of the protein and thus allows us to monitor the regulation of GQC substrates within the cell. Moreover, because GQC substrates are constitutively ubiquitinated, unlike PM permeases, this allows us to study VPS pathway regulation independently of the ubiquitination step.

Our results demonstrate that nutrient sensing regulates the delivery of GQC substrates to the vacuole via upregulation of the VPS pathway. This occurs in WT cells upon TOR inactivation and apparently in cells in which the selective endosome-Golgi retrieval pathway is blocked (e.g., *btn1Δ* and *btn2Δ* cells; Kama et al., 2007, 2011). Thus, alteration of endosome-Golgi trafficking might attenuate TOR signaling and thereby facilitate the targeting of Golgi proteins to the endolysosomal pathway. Because of the unrecognized role of starvation in GQC substrate delivery to the vacuole, some aspects of our earlier Btn2 work (Kama et al., 2007) may require reinterpretation. Therein, we described the delivery of GFP-Yif1 to the vacuole in *btn2Δ* cells grown and live-imaged on synthetic minimal medium, instead of the synthetic rich medium used here. This may have contributed to the vacuolar localization of GFP-Yif1. This does not call into question data showing Btn2 binding to GFP-Yif1, SNAREs, and retromer (Kama et al., 2007) or that GFP-Yif1 mislocalizes to endosomes in *btn1Δ* cells due to deficits in SNARE-dependent endosome-Golgi trafficking (Kama et al., 2011).

Overall, our study reveals an intersection between GQC and the MVB-VPS and TOR signaling pathways that control flux along the biosynthetic and endocytic route (Figure 7). The DSC complex was identified in *S. cerevisiae* but was uncharacterized in terms of function (Ryan et al., 2012). Large-scale screening identified potential Tul1 substrates in *S. cerevisiae* but did not reveal any commonalities between them (Tong et al., 2014). In contrast, the *S. pombe* DSC complex is proposed to ubiquitinate SREBP and promote proteasome cleavage, but this has not been connected to MVB protein sorting (Stewart et al., 2011). Since we show that the DSC complex is required for GQC in *S. cerevisiae*, this function may be conserved in *S. pombe*. To conclude, GQC substrate delivery to the vacuole upon AA starvation parallels the internalization and degradation of the PM nutrient-sensing machinery (e.g., permeases) and may be part of a general pre-autophagic response important for cell survival.

EXPERIMENTAL PROCEDURES

Media, DNA, and Genetic Manipulations

Yeast were grown on standard rich (YPD) or synthetic defined-rich media containing 2% glucose or 3.5% galactose at 26°C (Rose et al., 1990) prior to treatment. Nitrogen starvation medium (YNB-N; 0.17% yeast nitrogen base lacking AAs and ammonium sulfate, with 2% glucose) was prepared accordingly (Rose et al., 1990). Epitope-tagging of genomic loci was performed with specific primers to plasmids used as templates (Longtine et al., 1998). Gene deletion was performed by homologous recombination using PCR products flanking the appropriate genomic sequences. Strains are listed in Table S2. Plasmids are listed in Table S3. Genes were expressed from single-copy plasmids unless otherwise stated.

Microscopy and Labeling

For the visualization of fluorescent (e.g., GFP- and RFP-tagged) proteins (FPs), yeast were grown to mid-log phase at 26°C on synthetic-rich selective medium prior to imaging. For FM4-64 and FP co-labeling, yeast expressing a FP-tagged protein grown (as above) were incubated with FM4-64 (5.3 μM final concentration) for 0.5 hr. For starvation treatment (2 hr total) and FM4-64 labeling, yeast grown (as above) were shifted to AA starvation medium (YNB-N) for 1.5 hr prior to labeling with FM4-64 in the same medium for 0.5 hr. For rapamycin treatment (1 hr total) and FM4-64 labeling, yeast were grown (as above) and shifted for 0.5 hr to the same medium containing rapamycin (200 μg/l) prior to labeling with FM4-64 for 0.5 hr. Yeast were visualized in vivo using a Zeiss LSM780 confocal imaging system with a Plan Apochromat 63×/1.40 numerical aperture objective. Image acquisition and analysis was accomplished using the detection system and software provided by the manufacturer. Photoshop was used to assemble and size images for figures. Scale bars represent 5 μm. The average ± SD of three repetitive experiments was calculated for scoring cell labeling; 100 cells were scored for each condition per experiment.

Immunoprecipitation, Western Analysis, and Genetic Screening

Procedures for immunoprecipitation, western analysis, and the large-scale genetic screening of yeast are described in Supplemental Experimental Procedures.

SUPPLEMENTAL INFORMATION

Supplemental Information includes Supplemental Experimental Procedures, six figures, and three tables and can be found with this article online at http://dx.doi.org/10.1016/j.celrep.2015.08.026.

ACKNOWLEDGMENTS

We thank M. Babst, M. Glickman, R. Piper, and J. Valdez-Taubas for reagents; Z. Elazar and A. Navon for advice; L. Gal-Horowitz and V. Kanneganti for

technical support; and L. Haim-Vilmovsky. This work was supported by a fellowship to N.D. from the National Contest for Life (NCL)-Stiftung, Hamburg, Germany; grants to J.E.G. from the Israel Science Foundation (#358/10 and #717/14), State of Lower Saxony, Hannover, Germany, Jeanne & Joseph Nissim Foundation for Life Sciences Research, and the Miles and Kelly Nadal and Family Laboratory for Research in Molecular Genetics at the Weizmann Institute; and grants to M.S. from the European Union (ERCStG 260395). J.E.G. holds the Besen-Brender Chair in Microbiology and Parasitology.

Received: April 15, 2015
Revised: July 9, 2015
Accepted: August 9, 2015
Published: September 3, 2015

REFERENCES

Bilodeau, P.S., Urbanowski, J.L., Winistorfer, S.C., and Piper, R.C. (2002). The Vps27p Hse1p complex binds ubiquitin and mediates endosomal protein sorting. Nat. Cell Biol. *4*, 534–539.

Bilodeau, P.S., Winistorfer, S.C., Kearney, W.R., Robertson, A.D., and Piper, R.C. (2003). Vps27-Hse1 and ESCRT-I complexes cooperate to increase efficiency of sorting ubiquitinated proteins at the endosome. J. Cell Biol. *163*, 237–243.

Henne, W.M., Buchkovich, N.J., and Emr, S.D. (2011). The ESCRT pathway. Dev. Cell *21*, 77–91.

Hettema, E.H., Valdez-Taubas, J., and Pelham, H.R. (2004). Bsd2 binds the ubiquitin ligase Rsp5 and mediates the ubiquitination of transmembrane proteins. EMBO J. *23*, 1279–1288.

Hirano, S., Kawasaki, M., Ura, H., Kato, R., Raiborg, C., Stenmark, H., and Wakatsuki, S. (2006). Double-sided ubiquitin binding of Hrs-UIM in endosomal protein sorting. Nat. Struct. Mol. Biol. *13*, 272–277.

Hurley, J.H. (2008). ESCRT complexes and the biogenesis of multivesicular bodies. Curr. Opin. Cell Biol. *20*, 4–11.

Jones, C.B., Ott, E.M., Keener, J.M., Curtiss, M., Sandrin, V., and Babst, M. (2012). Regulation of membrane protein degradation by starvation-response pathways. Traffic *13*, 468–482.

Jung, C.H., Ro, S.H., Cao, J., Otto, N.M., and Kim, D.H. (2010). mTOR regulation of autophagy. FEBS Lett. *584*, 1287–1295.

Kama, R., Robinson, M., and Gerst, J.E. (2007). Btn2, a Hook1 ortholog and potential Batten disease-related protein, mediates late endosome-Golgi protein sorting in yeast. Mol. Cell. Biol. *27*, 605–621.

Kama, R., Kanneganti, V., Ungermann, C., and Gerst, J.E. (2011). The yeast Batten disease orthologue Btn1 controls endosome-Golgi retrograde transport via SNARE assembly. J. Cell Biol. *195*, 203–215.

Katzmann, D.J., Stefan, C.J., Babst, M., and Emr, S.D. (2003). Vps27 recruits ESCRT machinery to endosomes during MVB sorting. J. Cell Biol. *162*, 413–423.

Lauwers, E., Erpapazoglou, Z., Haguenauer-Tsapis, R., and André, B. (2010). The ubiquitin code of yeast permease trafficking. Trends Cell Biol. *20*, 196–204.

Longtine, M.S., McKenzie, A., 3rd, Demarini, D.J., Shah, N.G., Wach, A., Brachat, A., Philippsen, P., and Pringle, J.R. (1998). Additional modules for versatile and economical PCR-based gene deletion and modification in Saccharomyces cerevisiae. Yeast *14*, 953–961.

MacGurn, J.A., Hsu, P.C., Smolka, M.B., and Emr, S.D. (2011). TORC1 regulates endocytosis via Npr1-mediated phosphoinhibition of a ubiquitin ligase adaptor. Cell *147*, 1104–1117.

Morvan, J., Rinaldi, B., and Friant, S. (2012). Pkh1/2-dependent phosphorylation of Vps27 regulates ESCRT-I recruitment to endosomes. Mol. Biol. Cell *23*, 4054–4064.

Müller, M., Schmidt, O., Angelova, M., Faserl, K., Weys, S., Kremser, L., Pfaffenwimmer, T., Dalik, T., Kraft, C., Trajanoski, Z., et al. (2015). The coordinated action of the MVB pathway and autophagy ensures cell survival during starvation. eLife *4*, e07736.

Piper, R.C., and Luzio, J.P. (2007). Ubiquitin-dependent sorting of integral membrane proteins for degradation in lysosomes. Curr. Opin. Cell Biol. *19*, 459–465.

Raiborg, C., Wesche, J., Malerød, L., and Stenmark, H. (2006). Flat clathrin coats on endosomes mediate degradative protein sorting by scaffolding Hrs in dynamic microdomains. J. Cell Sci. *119*, 2414–2424.

Reggiori, F., and Pelham, H.R. (2002). A transmembrane ubiquitin ligase required to sort membrane proteins into multivesicular bodies. Nat. Cell Biol. *4*, 117–123.

Rose, M.D., Winston, F.M., and Heiter, P. (1990). Methods in yeast genetics: a laboratory course manual (Cold Spring Harbor, New York: Cold Spring Harbor Laboratory Press).

Ryan, C.J., Roguev, A., Patrick, K., Xu, J., Jahari, H., Tong, Z., Beltrao, P., Shales, M., Qu, H., Collins, S.R., et al. (2012). Hierarchical modularity and the evolution of genetic interactomes across species. Mol. Cell *46*, 691–704.

Sachse, M., Urbé, S., Oorschot, V., Strous, G.J., and Klumperman, J. (2002). Bilayered clathrin coats on endosomal vacuoles are involved in protein sorting toward lysosomes. Mol. Biol. Cell *13*, 1313–1328.

Seufert, W., and Jentsch, S. (1990). Ubiquitin-conjugating enzymes UBC4 and UBC5 mediate selective degradation of short-lived and abnormal proteins. EMBO J. *9*, 543–550.

Shestakova, A., Hanono, A., Drosner, S., Curtiss, M., Davies, B.A., Katzmann, D.J., and Babst, M. (2010). Assembly of the AAA ATPase Vps4 on ESCRT-III. Mol. Biol. Cell *21*, 1059–1071.

Shields, S.B., and Piper, R.C. (2011). How ubiquitin functions with ESCRTs. Traffic *12*, 1306–1317.

Stewart, E.V., Nwosu, C.C., Tong, Z., Roguev, A., Cummins, T.D., Kim, D.U., Hayles, J., Park, H.O., Hoe, K.L., Powell, D.W., et al. (2011). Yeast SREBP cleavage activation requires the Golgi Dsc E3 ligase complex. Mol. Cell *42*, 160–171.

Stringer, D.K., and Piper, R.C. (2011). A single ubiquitin is sufficient for cargo protein entry into MVBs in the absence of ESCRT ubiquitination. J. Cell Biol. *192*, 229–242.

Tong, Z., Kim, M.S., Pandey, A., and Espenshade, P.J. (2014). Identification of candidate substrates for the Golgi Tul1 E3 ligase using quantitative diGly proteomics in yeast. Mol. Cell. Proteomics *13*, 2871–2882.

Valdez-Taubas, J., and Pelham, H. (2005). Swf1-dependent palmitoylation of the SNARE Tlg1 prevents its ubiquitination and degradation. EMBO J. *24*, 2524–2532.

Wollert, T., and Hurley, J.H. (2010). Molecular mechanism of multivesicular body biogenesis by ESCRT complexes. Nature *464*, 864–869.

Wullschleger, S., Loewith, R., and Hall, M.N. (2006). TOR signaling in growth and metabolism. Cell *124*, 471–484.

Zhang, N., Quan, Z., Rash, B., and Oliver, S.G. (2013). Synergistic effects of TOR and proteasome pathways on the yeast transcriptome and cell growth. Open Biol. *3*, 120137.

Zhao, Y., Macgurn, J.A., Liu, M., and Emr, S. (2013). The ART-Rsp5 ubiquitin ligase network comprises a plasma membrane quality control system that protects yeast cells from proteotoxic stress. eLife *2*, e00459.